https://doi.org/10.5194/esurf-2021-1
Preprint. Discussion started: 22 January 2021

Earth Surface Dynamics Discussions
Open Access
EGU

A stream-power law for glacial erosion and its implementation in large-scale landform-evolution models

Stefan Hergarten[1]

[1]Institut für Geo- und Umweltnaturwissenschaften, Albert-Ludwigs-Universität Freiburg, Albertstr. 23B, 79104 Freiburg, Germany

Correspondence: Stefan Hergarten
(stefan.hergarten@geologie.uni-freiburg.de)

Abstract. Modeling glacial landform evolution is more challenging than modeling fluvial landform evolution. While several numerical models of large-scale fluvial erosion are available, there are only a few models of glacial erosion, and their application over long time spans requires a high numerical effort. In this paper, a simple formulation of glacial erosion which is similar to the fluvial stream-power model is presented. The model reproduces the occurrence of overdeepenings, hanging valleys, and steps at confluences at least qualitatively. Beyond this, it allows for a seamless coupling to fluvial erosion and sediment transport. The recently published direct numerical scheme for fluvial erosion and sediment transport can be applied to the entire domain, where the numerical effort is only moderately higher than for a purely fluvial system. Simulations over several million years on lattices of several million nodes can be performed on standard PCs. An open-source implementation is freely available as a part of the landform evolution model OpenLEM.

1 Introduction

Glaciers have played a major part in shaping several orogens on Earth. In contrast to fluvial erosion, however, glacial erosion has not been extensively considered in modeling large-scale landform evolution. The difference in mathematical and numerical complexity may be the main reason for this imbalance.

Models of large-scale fluvial landform evolution (for an overview, see, e.g., Willgoose, 2005; Wobus et al., 2006) are typically based on a simple expression for the erosion rate which dates back to studies of longitudinal river profiles by Hack (1957). This relation is often referred to as the stream-power law or as the stream-power incision model and considers the erosion rate E as a function of the upstream catchment size A and the channel slope S in the form

$$E = KA^m S^n. \tag{1}$$

All dependencies of E except for A and S are subsumed in the lumped parameter E, called erodibility. This also includes the geometry of the river's cross section, so that rivers can be considered as linear elements. The exponents m and n are believed to be more ore less universal. Equation (1) is occasionally written in the form

$$E = K\left(A^\theta S\right)^n \tag{2}$$

https://doi.org/10.5194/esurf-2021-1
Preprint. Discussion started: 22 January 2021


Earth Surface Dynamics Discussions
Open Access
EGU

with the concavity index $\theta = \frac{m}{n}$. In contrast to the absolute values of m and n, θ can be determined from the shape of longitudinal river profiles if the erosion rate is uniform along the river. Thus, the value of θ is well-constrained. Most modeling studies either use the value $\theta = 0.5$ originally found by Hack (1957) or a slightly lower reference value $\theta = 0.45$ (e.g., Whipple et al., 2013; Lague, 2014). Fully implicit schemes are available, where in principle arbitrarily large time increments can be used, while the numerical effort increases only linearly with the size of the grid (Hergarten and Neugebauer, 2001; Braun and Willett, 2013).

While the stream-power incision model is limited to scenarios where all material that is detached from the river bed is immediately excavated, some extensions towards sediment transport were developed. Recently, a generic formulation

$$\frac{E}{K_\mathrm{d}} + \frac{Q}{K_\mathrm{t} A} = A^m S^n, \tag{3}$$

called shared stream-power model, was presented (Hergarten, 2020), where Q is the sediment flux (volume per time). This model contains two parameters beyond the exponents m and n, where K_d describes the erodibility in the detachment-limited case and K_t the erodibility in the transport-limited case. Efficient numerical schemes for this model and the mathematically equivalent model of Davy and Lague (2009) have recently become available (Yuan et al., 2019; Hergarten, 2020). In particular, the direct solver introduced by Hergarten (2020) achieves almost the efficiency of the original stream-power incision model.

A comparable representation of glacial erosion where the erosion rate can be directly computed from properties of the topography is not yet available. Contemporary models involve at least the thickness of the ice layer and its velocity at each point of the topography. The shallow-ice approximation (Fowler and Larson, 1978; Hutter, 1980; Cuffey and Paterson, 2010) is widely used in this context. The flow follows the direction of the steepest descent of the ice surface, and the depth-averaged horizontal velocity is decomposed into a sliding velocity v_s and a deformation velocity v_d. Both velocity components depend on the on the thickness h of the ice layer and on the slope S of the ice surface according to the power-law relations

$$v_\mathrm{s} \sim h^{\psi-1} S^\psi \tag{4}$$

$$v_\mathrm{d} \sim h^{\psi+1} S^\psi, \tag{5}$$

where ψ is the exponent of Glen's flow law (typically $\psi \approx 3$, e.g., Cuffey and Paterson, 2010). The erosion rate is usually assumed to depend on the sliding velocity also by a power-law relation

$$E \sim v_s^l, \tag{6}$$

where the linear relation ($l = 1$) originally suggested by Hallet (1979) is still widely used.

The product of ice thickness and total velocity, $h(v_\mathrm{s} + v_\mathrm{d})$, defines the ice flux per unit width. Inserting this property into the mass balance of the glacier yields a differential equation for the thickness h. If the topography of the ice surface ($H + h$, where H is the topography of the bedrock) is considered as the variable, it is a diffusion equation with a high and strongly variable diffusivity. This property makes its numerical treatment challenging and allows only for small time increments.

The model ICE-CASCADE provided the first implementation of this concept in a large-scale landform evolution model (Braun et al., 1999). While this model has been applied in several studies, the iSOSIA (integrated Second-Order Shallow Ice

https://doi.org/10.5194/esurf-2021-1
Preprint. Discussion started: 22 January 2021


Earth Surface Dynamics Discussions
Open Access
EGU

Approximation) model introduced by Egholm et al. (2011) is a step towards a more realistic description of ice flow without solving the full three-dimensional equations of flow. As a major point, it also takes into account longitudinal and transverse stresses, which impedes strong local gradients in ice velocity and the incision into the bedrock along thin lines. This problem had to be fixed in ICE-CASCADE by a more heuristic approach based on the curvature of the topography. However, both models still require small time increments and are computationally expensive.

2 A stream-power law for glacial erosion

According to Eqs. (4) and (5), the ratio of v_d and v_s is proportional to h^2. Thus, the relative contribution of deformation to the total flux converges to zero in the limit of a thin layer, provided that the ice is not frozen to the bedrock. So let us assume for the moment that the entire ice flux is dominated by sliding. If we consider a rectangular cross section of a width w, the total ice flux (volume per time, not per unit width) is

$$q_\mathrm{i} = whv_\mathrm{s}. \tag{7}$$

The thickness h can be eliminated by combining Eqs. (4) and (7), which yields

$$v_\mathrm{s} \sim \left(\frac{q_\mathrm{i}}{w}\right)^{\frac{\psi-1}{\psi}} S. \tag{8}$$

Then the erosion rate (Eq. 6) is

$$E \sim \left(\left(\frac{q_\mathrm{i}}{w}\right)^{\frac{\psi-1}{\psi}} S\right)^l. \tag{9}$$

In order to obtain an expression similar to the fluvial stream-power law (Eq. 1 or 2), we need an estimate of the width w. In the 1D model of Prasicek et al. (2020) with a dendritic glacier network, the width was expressed in terms of the upstream flow length. This approach was justified by results of Bahr (1997) who found a power-law relationship

$$w \sim L^\chi \tag{10}$$

with $\chi = 0.6$, where w is the mean width and L the total length of the glacier. Prasicek et al. (2020) obtained the same relationship with a slightly lower exponent of $\chi = 0.58$ from an analysis of 52,000 glacier polygons. Equation (10) cannot be transferred directly to the width at any point and the upstream flow length at this point. However, if we assume that it holds for each point in terms of actual width and upstream flow length, it is also valid for the mean width and the total flow length. So it makes sense to follow the concept proposed by Prasicek et al. (2020) and assume that Eq. (10) holds for each point. In the same study, it was also found that glaciers follow the fundamental relationship

$$L \sim A^\eta \tag{11}$$

originally proposed by Hack (1957) for rivers, although with a slightly lower exponent η. While Hack (1957) found $\eta = 0.6$ and a later, more comprehensive study of Rigon et al. (1996) $\eta = 0.56$, Prasicek et al. (2020) obtained $\eta = 0.52$ from the drainage

https://doi.org/10.5194/esurf-2021-1
Preprint. Discussion started: 22 January 2021


Earth Surface Dynamics Discussions
Open Access
EGU

pattern of a previously glaciated region, suggesting that glacier patterns are more straight than rivers. Combining Eqs. (10) and (11) yields

$$w \sim A^{\alpha}, \tag{12}$$

where $\alpha = \chi h \approx 0.30$ with the values suggested by Prasicek et al. (2020). If we assume a constant rate of ice production over the entire upstream catchment for the moment, q_i is proportional to A, and thus

$$w \sim q_\mathrm{i}^{\alpha}. \tag{13}$$

Then the erosion rate (Eq. 9) turns into

$$E \sim \left(q_\mathrm{i}^{\theta_\mathrm{g}} S\right)^{l} \tag{14}$$

with

$$\theta_\mathrm{g} = (1-\alpha)\,\frac{\psi - 1}{\psi}. \tag{15}$$

Equation (14) has the same shape as Eq. (2), where l takes the role of n. So Eq. (14) can be interpreted as a stream-power law for glacial erosion.

The glacial concavity index θ_g is about 0.47 for $\psi = 3$, which is strikingly close to the widely used values $\theta = 0.45$ or $\theta = 0.5$ for fluvial erosion. The estimate of θ_g is, however, exposed to a higher uncertainty not only because the width-scaling exponent α is based on simple assumptions, but also because there is a considerable uncertainty about the value of ψ. This finding suggests to assume $\theta_\mathrm{g} = \theta$, which also facilitates the interpretation of the factor of proportionality in Eq. (14).

The main difference between Eq. (14) and Eq. (2) is that the latter is written in terms of catchment size instead of flux for historical reasons. The erodibility K is a lumped parameter that already includes precipitation. If we assume that a given erodibility K refers to a uniform reference precipitation p_0, the long-term mean discharge from a catchment of size A is $q = p_0 A$. If we further take into account that erosion rather depends on discharge than on catchment size, Eq. (2) written in terms of q instead of A should also be applicable to non-uniform precipitation. Let us, for convenience, express the discharge as a catchment-size equivalent by defining

$$A = \frac{q}{p_0}. \tag{16}$$

Then all relations remain formally the same with the discharge measured in catchment-size equivalents. The ice flux q_i can also be measured as a catchment-size equivalent according to

$$A_\mathrm{i} = \frac{q_\mathrm{i}}{p_0}. \tag{17}$$

We can then write Eq. (14) in the same form as Eq. (2),

$$E = K_\mathrm{g} \left(A_\mathrm{i}^{\theta} S\right)^{l}. \tag{18}$$

https://doi.org/10.5194/esurf-2021-1
Preprint. Discussion started: 22 January 2021


Earth Surface Dynamics Discussions
Open Access
EGU

If we take into account that both exponents l and n are not well-constrained and assume $l = n$, the erodibilities K_g and K have the same meaning and the same physical unit. So the glacial stream-power law defined by Eq. (18) subsumes the physical and climatic parameters of the ice flux (Eq. 4) and glacial erosion (Eq. 6) to a single lumped parameter K_g. The glacial stream-power law can then be written in the same form as Eq. (1),

$$E = K_\mathrm{g} A_\mathrm{i}^m S^n, \tag{19}$$

where the exponents m and n are the same as for fluvial erosion.

3 Implementation in a landform evolution model

The glacial stream-power model developed in the previous section considers glaciers as linear elements. Since Eq. (19) refers to the total ice flux through the entire cross section area and not to a flux per unit width, the glacier should be described by a cardinal flow line instead of a parallel flow pattern. So let us start from a dendritic flow pattern on a discrete lattice as typically used in large-scale fluvial landform evolution models. Each cell of the grid has a unique flow direction towards the neighbor with the steepest descent, and the respective slope defines the channel slope S.

Let us assume steady-state conditions for the fluxes of water and ice, although this is, strictly speaking, not justified for the ice if the climate changes rapidly. The total flux A (water and ice) and the ice flux A_i (both measured in terms of catchment-size equivalent) are then given by the steady-state balance equations

$$A = s\frac{p}{p_0} + \sum_{\text{donors}} A, \tag{20}$$

$$A_\mathrm{i} = s\frac{p_\mathrm{i}}{p_0} + \sum_{\text{donors}} A_\mathrm{i}, \tag{21}$$

where p is the total precipitation, p_i is the part of p that is converted into ice, and s is the pixel area of the considered grid cell. The sum extends over all neighbors that deliver their discharge to the considered site, called donors in the following.

This concept is widely used in modeling fluvial erosion. However, the spatial scales are different here. At least small rivers are usually narrower than the mesh width of the lattice. As this may cause problems for detachment-limited erosion in combination with hillslope processes, approaches taking into account that rivers cover only a part of the pixels of the grid were developed (Howard, 1994; Perron et al., 2008; Pelletier, 2010). Glaciers are, however, often wider than typical mesh widths of some tens to hundreds of meters. Thus, glacial erosion acts over an area around to the cardinal flow path, called swath in the following. The scaling arguments developed in the previous section suggest that the width of the swath is a function of the ice flux according to Eq. (12). This concept is in principle the same as following the cardinal flow path with a pen of a variable width w.

Since Eq. (19) only describes the erosion rate at the cardinal flow path, an assumption must be made for the other points of the swath. One might think of prolonging either the surface height or the erosion rate from the cardinal flow directly. However, both ideas are unrealistic end-members where one transforms each valley into a perfect U-valley immediately, and the other one is unable to change the cross-sectional shape of a valley at all. A prolongation of the ice flux A_i used in Eq. (19) is a more realistic approach. Then the erosion rate of the points on the swath is the same as on the cardinal flow line if the channel slope

https://doi.org/10.5194/esurf-2021-1
Preprint. Discussion started: 22 January 2021

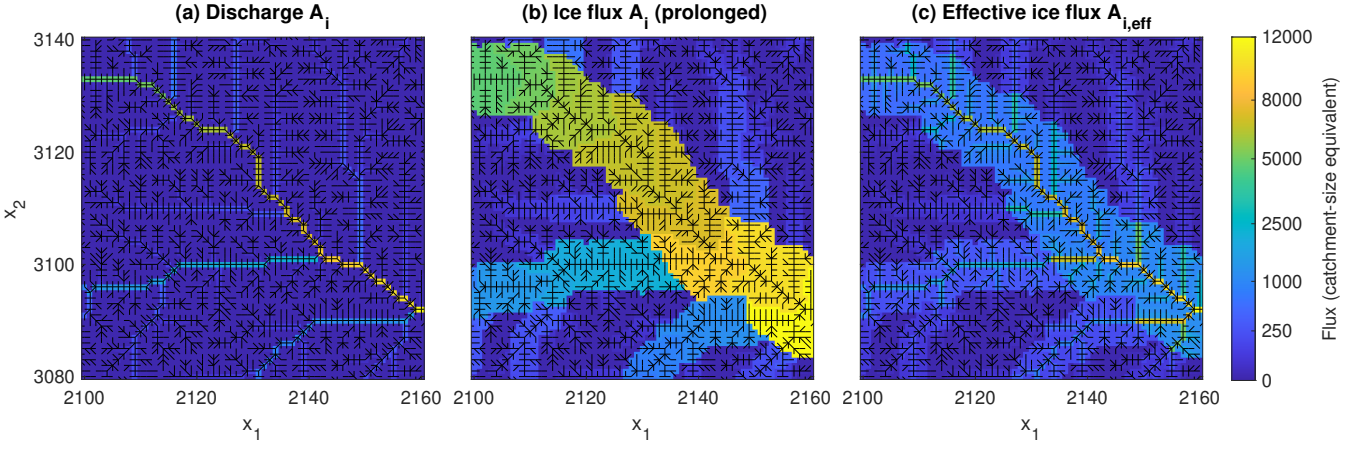

Figure 1. Illustration of the fluxes in the swath around the cardinal flow path. The domain corresponds to the small, white square in Fig. 2.

is the same. Over long times, the topography of the valley floor will adjust in such a way that the local channel slope of all points is the same as on the cardinal flow line.

The algorithm used for swath profiles across a given baseline based on the minimum distance (Hergarten et al., 2014) could be used for drawing the swath and for assigning a reference point on the cardinal flow line to each point of the swath. In this study, however, a slightly different approach based on catchments is suggested.

Let c_0 be a point on the cardinal flow path, and c_i for $i \geq 1$ the upstream points on the cardinal flow path, defined by the condition that c_{i+1} is the biggest donor of c_i. Let u be any donor of c_0, which is not on the cardinal flow path ($u \neq c_1$). The point u is added to the swath and assigned to c_0 if the distance between u and c_i is not greater than $\frac{w_i}{2}$ for any $i \geq 0$, where w_i is the width according to Eq. (12) applied to the ice flux of the point c_i. After selecting the donors of c_0 that satisfy this condition, the same procedure is applied to all donors of these points. The procedure continues until no more donors that satisfy the condition are found.

However, there is no straightforward definition of cardinal flow lines on an absolute scale since dendritic flow patterns may cover a wide range of scales. Therefore, the procedure described above is applied to all points c_0 with a nonzero ice flux. Finally, the largest value of A_i (resulting from different starting points c_0) is taken for each point.

An example of the obtained swaths and the respective fluxes is shown in Fig. 1. The topography used here is a fluvial equilibrium topography with $K = 1$, $m = 0.5$, and $n = 1$ under uniform uplift $U = 1$ on a grid of 5000×5000 nodes. This topography is shown in Fig. 2. It was already used by Hergarten (2020, Fig. 1a), where the only difference is a shift of the periodic eastern and western boundaries in such a way that the three biggest rivers do not cross the boundaries.

However, this approach is not free of problems. Since parts of the swath have the same ice flux, flow parallel to the cardinal flow line is preferred over a dendritic flow pattern towards this line. Flow parallel to the cardinal flow path does not contribute to the flux at the cardinal flow path and thus reduces this flux artificially. Since the glacial stream-power law (Eq. 19) refers to the total ice flux and not to the flux per unit, parallel flow also reduces the erosion rate artificially. The problem is basically the

https://doi.org/10.5194/esurf-2021-1
Preprint. Discussion started: 22 January 2021

Earth Surface Dynamics Discussions
Open Access
EGU

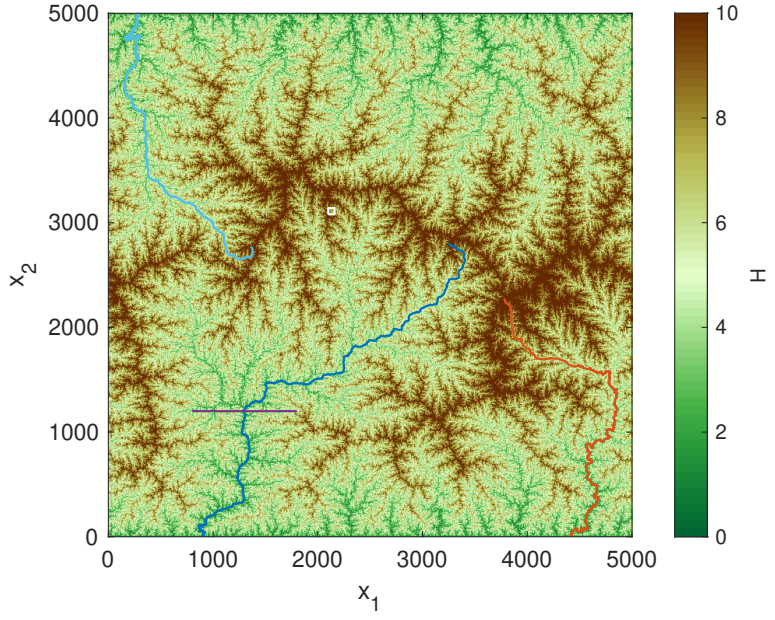

Figure 2. Fluvial equilibrium topography under uniform uplift (Hergarten, 2020, Fig. 1a). The small, white square depicts the domain of Fig. 1. The blue and red lines show the three biggest rivers. The violet line refers to the profile shown in Fig. 4.

same as for the runoff of water on hillslopes where the transition from parallel flow to channelized flow was addressed, e.g., by Pelletier (2010).

In order to overcome this problem, the prolongation from the cardinal flow line to the swath should be defined in such a way that dendritic flow patterns towards the cardinal flow line are still maintained. In the following, an effective ice flux obtained from a weighted geometric mean value

$$A_{\mathrm{i,eff}} = A^{\epsilon}\, A_{\mathrm{i}}^{1-\epsilon} \tag{22}$$

is used in the glacial stream-power law, where A_{i} is the prolonged ice flux. The parameter ϵ defines the weighting of the two fluxes. Larger values of ϵ provide a better suppression of parallel flow patterns, but in turn make glacial valleys more V-shaped. In all numerical simulations performed during the preparation of this paper, $\epsilon = 0.25$ turned out to be a safe choice.

As a first example, Fig. 3 shows a steady-state glacial topography for $K_{\mathrm{g}} = 1$. It was assumed that the entire precipitation is converted into ice ($p_{\mathrm{i}} = p = p_0$). The factor of proportionality in Eq. (12) was set to unity (in units of the grid spacing), so $w = A_{\mathrm{i}}^{0.3}$. The term steady state is seen in a loose sense here. After simulating a time span of 25 time units starting from the fluvial equilibrium topography, both the maximum and the mean surface height show no systematic trend any more, although they still oscillate due to local reorganization of the drainage pattern. Obtaining a steady state in the strict sense would, if possible at all, require a much longer time period, but this is not relevant for this study.

As expected, a strong downstream increase in valley width is the main difference towards the fluvial equilibrium topography. Due to the U-shape of the big valleys, the parts of the tributaries that are captured by the swath are almost flat, which is

https://doi.org/10.5194/esurf-2021-1
Preprint. Discussion started: 22 January 2021

Earth Surface Dynamics Discussions
Open Access
EGU

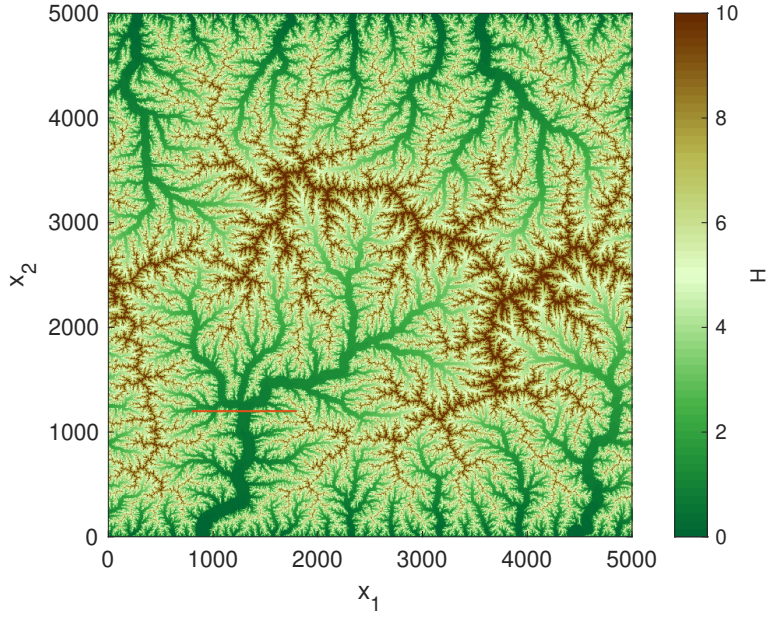

Figure 3. Glacial equilibrium topography under uniform uplift with the entire precipitation converted into ice. The red line refers to the profile shown in Fig. 4.

equivalent to lowering their base level compared to the fluvial topography. As a consequence, the surface heights of high regions decrease, although the same erodibility as for fluvial erosion was assumed.

Both the occurrence of wide, U-shaped valleys and the reduced elevation are also visible in the topographic profiles shown in Fig. 4. Beyond these, the slight V-shape of the valley floors arising from Eq. (22) is also visible. If we assume a typical grid spacing of 50 m, the largest valley is about 6 km wide. The maximum surface height over the entire domain is about 16. If we assume that it amounts to 4000 m in reality, one vertical length unit is equivalent to 250 m. The height difference across the largest valley is about 0.08, corresponding to about 20 m. So the across-valley slope of this valley is about 0.3 %. Smaller valleys, however, have a stronger residual V-shape. The valleys around $x_1 = 1000$ and $x_1 = 1500$, e.g., have across-valley slopes between 2 % and 6 %.

4 Fluvio-glacial systems

The ratio of p_i and p typically decreases with decreasing altitude. The equilibrium line altitude (ELA) defines the height where $p_\mathrm{i} = 0$. Below the ELA, melting dominates, so p_i is negative. Somewhere below the ELA, melting even compensates the contribution of tributaries, resulting in a downstream decrease in A_i.

A simple, linear model for the part of the total precipitation that is converted into ice,

$$p_\mathrm{i} = p \min\left(\frac{H - H_\mathrm{e}}{H_\mathrm{f} - H_\mathrm{e}}, 1\right), \tag{23}$$

https://doi.org/10.5194/esurf-2021-1
Preprint. Discussion started: 22 January 2021

Earth Surface Dynamics Discussions
Open Access
EGU

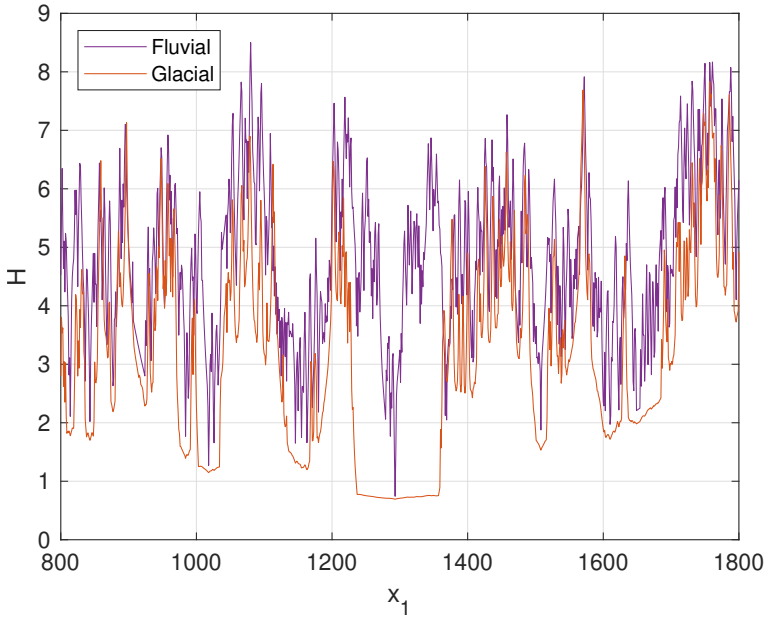

Figure 4. Topographic profiles along the lines depicted in Figs. 2 and 3.

is used in this study, where H_e is the ELA and H_f is the altitude where the entire precipitation is converted into ice. The surface height H cannot be included easily in the fully implicit scheme for erosion, so it is evaluated at the beginning of the time step. This will, however, not strongly affect the stability of the implicit scheme and is a minor restriction of the maximum time increment compared to treating the flow directions in an explicit manner (Hergarten, 2020).

Figure 5 shows an example of the total flux and the ice flux of the three largest rivers from Fig. 2 for $H_e = 8$ and $H_f = 10$, corresponding to 2000 m and 2500 m, respectively, using the vertical scale defined above. Practically, A_i is still not much lower than A at the ELA. The point of maximum ice flux is found below the ELA due to the ice flux of tributaries. At this point, A is already more then three times greater than A_i for the considered flow paths. This means that the discharge of water is considerably higher than the ice flux for a major part of the flow path.

Assuming that all sites with $A_i > 0$ are eroded glacially, while fluvial erosion only affects ice-free sites, is the simplest concept of a coupled model. While this concept was used by Prasicek et al. (2020), the following example illustrates that it may cause problems when applied over long time spans.

Figure 6 shows a topography obtained for $H_e = 8$ and $H_f = 10$, where the glacial erodibility, $K_g = 2$, is twice the fluvial erodibility ($K = 1$). While the initial state (fluvial equilibrium) and the simulated time span ($t = 25$) are the same as for the example with full glaciation (Fig. 3), the topography is still far off from a steady state here.

Profiles along the three largest flow paths marked in Fig. 6 are depicted in Fig. 7 (lower solid lines). All profiles show a quite steep increase at the glacier terminus, which may even be a sharp front. This steep front is is not a specific property of the stream-power approach proposed here, but was already visible in the steady-state topographies obtained by Prasicek et al.

https://doi.org/10.5194/esurf-2021-1
Preprint. Discussion started: 22 January 2021

Earth Surface Dynamics Discussions
Open Access
EGU

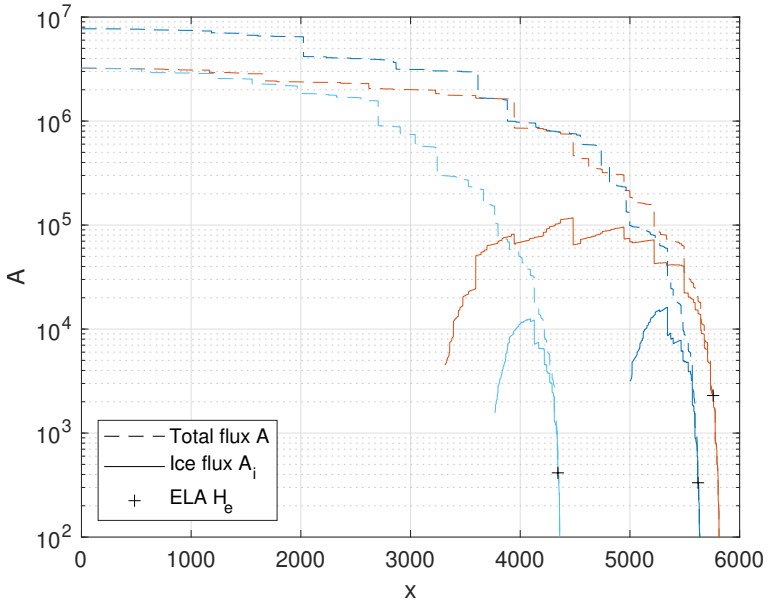

Figure 5. Total flux A and ice flux A_i of the flow paths shown in Fig. 2 for $H_\mathrm{e} = 8$ and $H_\mathrm{f} = 10$.

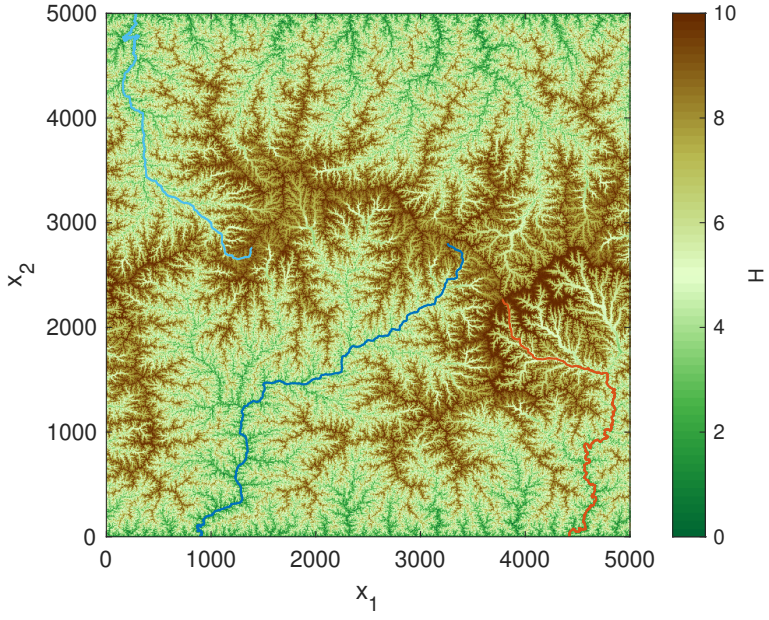

Figure 6. Topography at $t = 25$ for $H_\mathrm{e} = 8$, $H_\mathrm{f} = 10$, $K_\mathrm{g} = 2$, and $K = 1$.

(2020, Figs. 5 and 7). It occurs because the ice flux approaches zero close to the glacier terminus. In this situation, a nonzero

https://doi.org/10.5194/esurf-2021-1
Preprint. Discussion started: 22 January 2021

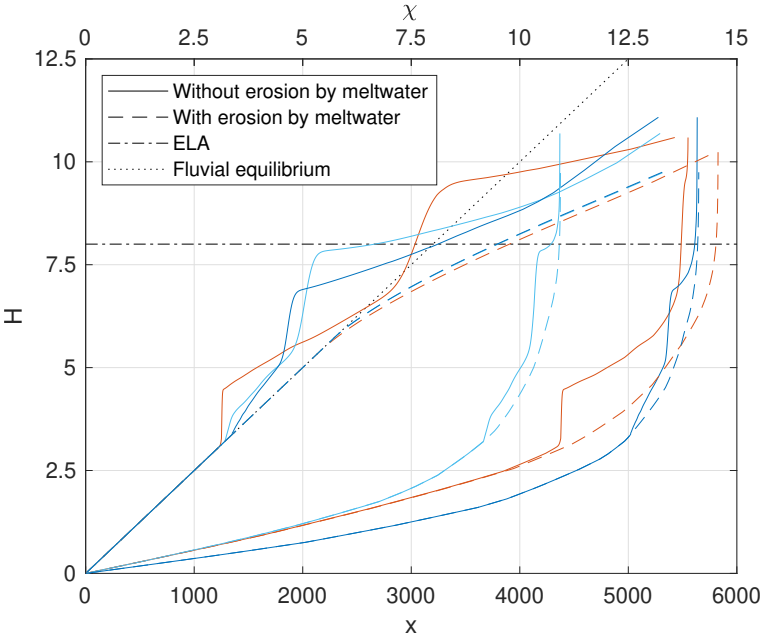

Figure 7. Longitudinal profiles of the largest flow paths in the fluvio-glacial topographies shown in Fig. 6 (solid lines) and Fig. 8 (dashed lines). The lower set of lines refers to the original longitudinal coordinate x, while the upper set of lines depicts the χ-transformed profiles.

erosion rate can only be achieved if $S \to \infty$ at the glacier terminus. In the dynamic model considered here, the glacier terminus migrates, which leads to an upstream propagation of steep segments, similarly to the propagation of knickpoints in rivers.

The χ transform introduced by Perron and Royden (2013) provides a simple way to analyze longitudinal river profiles quantitatively. It transforms the upstream coordinate x to a new coordinate

$$\chi = \int A(x)^{-\theta} dx. \tag{24}$$

The χ transform eliminates the inherent concavity of river profiles arising from the upstream decrease in catchment size. Equilibrium profiles under spatially uniform conditions turn into straight lines with a slope of $\left(\frac{U}{K}\right)^{\frac{1}{n}}$. In our example ($K = 1$, $U = 1$), it is even the diagonal line $H = \chi$.

The upper solid lines in Fig. 7 depict the χ-transformed profiles. The plot reveals that the profiles are even steeper than the fluvial part on average almost up to the ELA. So the lower ice flux compared to the total discharge even shadows the higher glacial erodibility here. This effect could be compensated by increasing the glacial erodibility further, but the rather unrealistic steep fronts in the bedrock topography would persist.

These findings support the idea that erosion by meltwater must play an important role, at least in the lower part of glaciers where the flux of water is much higher than the ice flux. The iSOSIA model was already extended by transport-limited erosion by meltwater quite soon (Egholm et al., 2012). While Beaud et al. (2016) developed a more elaborate model for the incision by meltwater within narrow channels, the meltwater component should preferably not introduce a level of complexity much

https://doi.org/10.5194/esurf-2021-1
Preprint. Discussion started: 22 January 2021


Earth Surface Dynamics Discussions
Open Access
EGU

beyond the simple models of fluvial and glacial erosion used here. So let us assume that erosion by meltwater can be described by the same formalism as fluvial erosion. The respective form of Eq. (1), reads

$$E = K_{\mathrm{f}} \left(A - A_{\mathrm{i}}\right)^m S^n, \tag{25}$$

where K_{f} was used instead of K, and the catchment-size equivalent of the meltwater flux is $A - A_{\mathrm{i}}$. Adding the glacial erosion rate (Eq. 19) and the meltwater erosion rate (Eq. 25) yields

$$E = K_{\mathrm{g}} A^m S^n + K_{\mathrm{f}} \left(A - A_{\mathrm{i}}\right)^m S^n. \tag{26}$$

This expression can be written conveniently in the form of Eq. (1) or Eq. (19),

$$E = K_{\mathrm{eff}} A^m S^n, \tag{27}$$

with the effective erodibility

$$K_{\mathrm{eff}} = \gamma^m K_{\mathrm{g}} + (1-\gamma)^m K_{\mathrm{f}}, \tag{28}$$

where

$$\gamma = \frac{A_{\mathrm{i}}}{A} \tag{29}$$

is the relative contribution of ice to the total flux.

Figure 8 shows a fluvio-glacial equilibrium topography obtained under the same conditions as the previous example, but including erosion by meltwater. Since there is no discontinuity in the erosion rate at the glacier terminus then, the changes in the flow pattern are much smaller than for the version without erosion by meltwater. The respective profiles depicted in Fig. 7 (dashed lines) reveal a smooth transition from the glacial regime to the fluvial regime. As expected, the χ-transformed profiles follow a straight line with a slope of 0.5 in the glacial domain, corresponding to the erodibility $K_{\mathrm{g}} = 2$ in equilibrium. So the higher glacial erodibility indeed leads to lower surface heights in the upper regions in contrast to the version without erosion by meltwater.

In the simple version presented above, it is assumed that the entire discharge except for the part that is ice contributes to fluvial erosion. As discussed, e.g., by Egholm et al. (2012), this may not be realistic. At least if the ice layer is thick, only a part of the runoff reaches the bedrock and can contribute to erosion. This could be easily taken into account by multiplying the term $A - A_{\mathrm{i}}$ in Eqs. (25) and (26) by a factor $\omega \in [0,1]$. This modification results in a factor ω in front of the term $1-\gamma$ in Eq. (28) and in all occurrences of this term in the following sections. The factor ω, however, is probably not constant over the entire glacier, but should decrease with increasing ice thickness. In order to avoid a discontinuity at the glacier terminus, it should approach unity there.

While the technical implementation would be simple if a model for the factor ω is given, it is not considered as an essential part of the model proposed in this study and is therefore not considered further.

https://doi.org/10.5194/esurf-2021-1
Preprint. Discussion started: 22 January 2021

Earth Surface Dynamics Discussions
Open Access
EGU

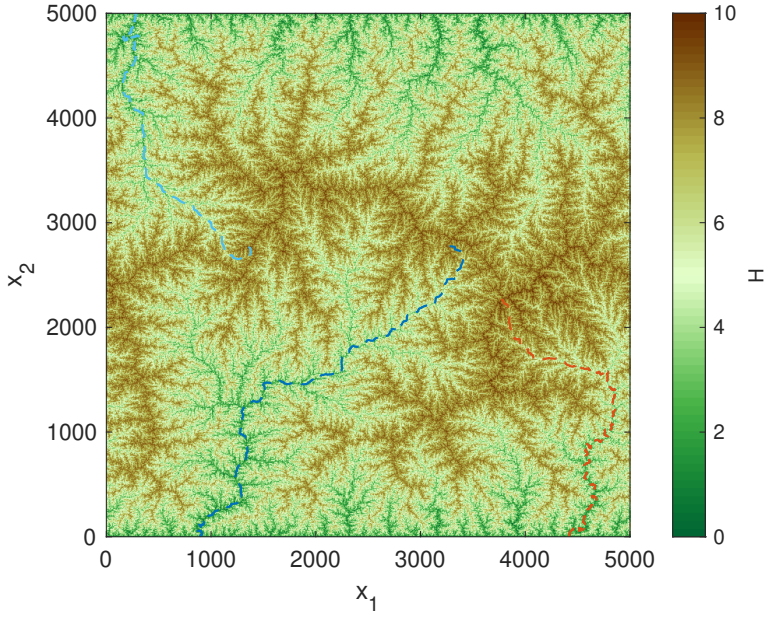

Figure 8. Topography obtained under the same conditions as in Fig. 6, but assuming that erosion by meltwater follows the same relation as fluvial erosion with the same erodibility.

5 Sediment transport

The shared stream-power model (Eq. 3) provides a simple formulation for the entire range between the detachment-limited and transport-limited end-members. Let us assume that the identical relations for glacial and fluvial erosion do not only hold for the detachment-limited end-member, and that the shared stream-power model provides a reasonable description of both glacial erosion and erosion by meltwater. Writing Eq. (3) individually for the ice and the meltwater components yields

$$\frac{E_\mathrm{g}}{K_\mathrm{d,g}} + \frac{Q_\mathrm{g}}{K_\mathrm{t,g} A_\mathrm{i}} = A_\mathrm{i}^m S^n, \tag{30}$$

$$\frac{E_\mathrm{f}}{K_\mathrm{d,f}} + \frac{Q_\mathrm{f}}{K_\mathrm{t,f} (A - A_\mathrm{i})} = (A - A_\mathrm{i})^m S^n. \tag{31}$$

The additional indices g and f refer to the glacial and fluvial (meltwater) component, respectively. So there are four erodibilities now, referring to glacial and fluvial incision and transport, respectively.

Since the flow of meltwater should be confined to narrow channels, the best approach would be to consider the two sediment fluxes Q_g and Q_f as separate variables without any mixing. The numerical scheme proposed by Hergarten (2020) could in principle be extended accordingly. However, this would require additional theoretical and numerical effort. Beyond this, the two sediment fluxes merge anyway, e.g., if material is deposited by the glacier due to decreasing transport capacity when approaching the glacier terminus and eroded again by the meltwater stream. Therefore, a simpler approach using a single

https://doi.org/10.5194/esurf-2021-1
Preprint. Discussion started: 22 January 2021


Earth Surface Dynamics Discussions
Open Access
EGU

sediment flux is suggested. According to Eqs. (30) and (31), the total erosion rate $E = E_\mathrm{g} + E_\mathrm{f}$ follows the relation

$$E + \frac{K_\mathrm{d,g} Q_\mathrm{g}}{K_\mathrm{t,g} \gamma A} + \frac{K_\mathrm{d,f} Q_\mathrm{f}}{K_\mathrm{t,f} (1-\gamma) A} = K_\mathrm{d,eff} A^m S^n, \tag{32}$$

where the definition of the effective erodibility for incision,

$$K_\mathrm{d,eff} = \gamma^m K_\mathrm{d,g} + (1-\gamma)^m K_\mathrm{d,f}, \tag{33}$$

is the same as in Eq. (28). If the total sediment flux $Q = Q_\mathrm{g} + Q_\mathrm{f}$ is given, the fraction of the stream power spent for sediment transport depends on how Q is distributed. Let us assume an optimized distribution in the sense that this fraction is minimized. It is easily recognized that this is the case if either the glacier or the meltwater carries the entire load, and thus

$$E + \min\left(\frac{K_\mathrm{d,g}}{K_\mathrm{t,g} \gamma}, \frac{K_\mathrm{d,f}}{K_\mathrm{t,f} (1-\gamma)} \right) \frac{Q}{A} = K_\mathrm{d,eff} A^m S^n. \tag{34}$$

This equation can be written in the same form as the original shared stream-power model (Eq. 3),

$$\frac{E}{K_\mathrm{d,eff}} + \frac{Q}{K_\mathrm{t,eff} A} = A^m S^n, \tag{35}$$

with

$$K_\mathrm{t,eff} = K_\mathrm{d,eff} \max\left(\gamma \frac{K_\mathrm{t,g}}{K_\mathrm{d,g}}, (1-\gamma) \frac{K_\mathrm{t,f}}{K_\mathrm{d,f}} \right). \tag{36}$$

Figures 9 and 10 provide a numerical example. Since sediment transport is more interesting in transient states than in a steady state, a declining ELA was chosen here. The ELA starts from $H_\mathrm{e} = 16$ (slightly higher than the maximum surface height of the fluvial equilibrium topography) and decreases at a rate of 4 (four times faster than the uplift), so that an ELA of $H_\mathrm{e} = 8$ (and $H_\mathrm{f} = 10$) is reached at $t = 2$.

The fluvial erodibilities are set to $K_\mathrm{d,f} = 2.6$ and $K_\mathrm{t,f} = 1.625$. Their ratio is $\frac{K_\mathrm{d,f}}{K_\mathrm{t,f}} = 1.6$. This ratio is the sediment deposition coefficient in the notation of Davy and Lague (2009), where a recent analysis of steady-state topographies suggested 1.6 as a realistic value for $n = 1$ (Guerit et al., 2019, data supplement). Furthermore, these values satisfy the relation

$$\frac{1}{K_\mathrm{d,f}} + \frac{1}{K_\mathrm{t,f}} = \frac{1}{K_\mathrm{f}} \tag{37}$$

with $K_\mathrm{f} = 1$, which ensures that the fluvial equilibrium topography computed for the detachment-limited model is also in equilibrium here (Hergarten, 2020). For glacial erosion, it is assumed that bedrock incision is not more efficient as fluvial bedrock incision ($K_\mathrm{d,g} = K_\mathrm{d,f} = 2.6$), while the glacier transports sediment 10 times more efficiently than water ($K_\mathrm{t,g} = 10 K_\mathrm{t,f} = 16.25$).

While the topography (Fig. 9) is similar to the topography shown in Fig. 8, the longitudinal profiles (Fig. 10) show distinct differences to the detachment-limited version. First, the fluvial parts of the profiles have become steeper compared to the initial fluvial topography. This increase in steepness is due to the high sediment flux from the glaciated part. As the erosion rate in the glacial part is higher than in equilibrium, the glacier brings more sediment than the upstream part of the river brought under

https://doi.org/10.5194/esurf-2021-1
Preprint. Discussion started: 22 January 2021

Earth Surface Dynamics Discussions
Open Access
EGU

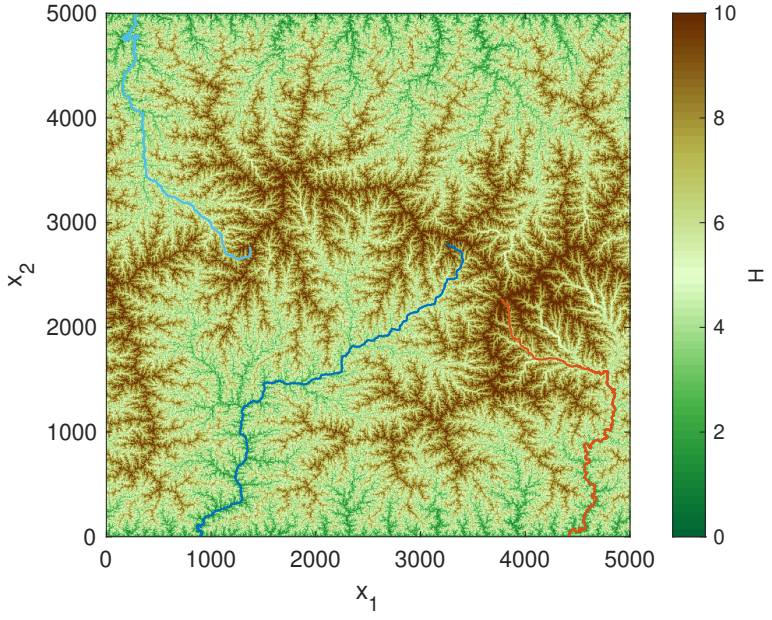

Figure 9. Topography obtained from the shared stream-power model at the time when the ELA reaches $H_e = 8$.

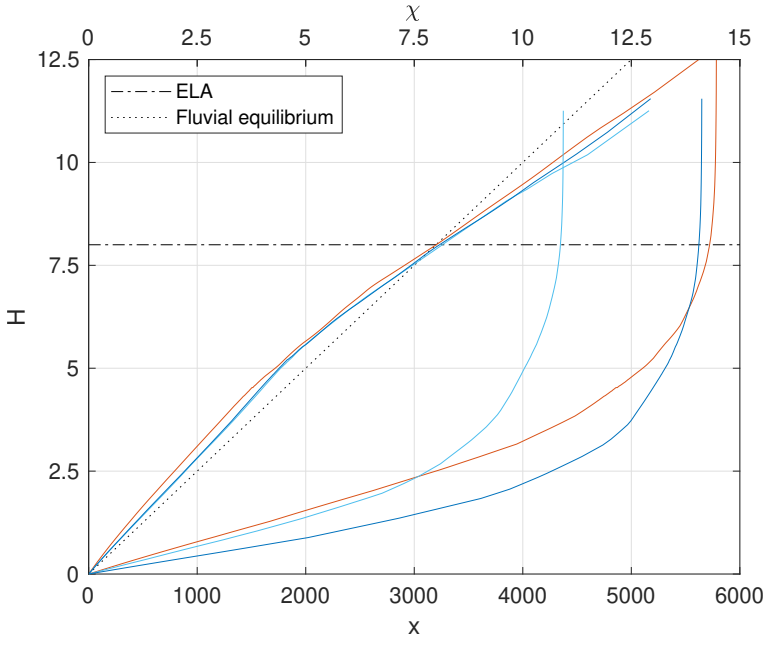

Figure 10. Longitudinal profiles of the largest flow paths in the topography shown in Fig. 9. The lower set of lines refers to the original longitudinal coordinate x, while the upper set of lines depicts the χ-transformed profiles.

https://doi.org/10.5194/esurf-2021-1
Preprint. Discussion started: 22 January 2021


Earth Surface Dynamics Discussions
Open Access
EGU

fluvial conditions. This increased sediment flux reduces the ability to erode the bedrock according to Eq. (3), and the fluvial erosion cannot follow the uplift any more.

The glaciated parts of the profiles are less steep than the initial fluvial profiles, but still steeper than it would be expected in equilibrium. Their slope in the χ plot is about 0.8, while Eq. (37) predicts an equilibrium slope of $\frac{1}{K_{\mathrm{d,g}}} + \frac{1}{K_{\mathrm{t,g}}} = 0.45$ with the glacial erodibilities assumed here. So the glaciated part is even steeper than the fluvial part if both are considered in relation to their equilibrium slope. The reason for the increased steepness is basically the same as for the fluvial part. Converting a V-shaped valley into a U-shaped valley goes along with a high erosion rate and thus yields a high amount of sediment. Although the efficiency of the glacier in transporting sediment was assumed to be ten times higher than for the rivers, the large amount of sediments limits the ability of the glacier to erode the bedrock during the conversion of the valley shape.

6 Finite ice thickness

The approach developed in Sect. 2 considers the limit of zero ice thickness. The finite thickness, however, has a strong influence on glacial landform evolution. Overdeepened valleys would be neither possible in the stream-power model proposed here nor in the original shallow-ice approximation in the limit of zero thickness. Beyond this, the ice surface defines a base level for the tributaries and may thus play an important part in the formation of hanging valleys.

A first estimate of the thickness h can be obtained by combining Eqs. (7) and (8) in the form

$$q_{\mathrm{i}} \sim wh \left(\frac{q_{\mathrm{i}}}{w}\right)^{\frac{\psi-1}{\psi}} S, \tag{38}$$

and thus

$$h \sim \left(\frac{q_{\mathrm{i}}}{w}\right)^{\frac{1}{\psi}} S^{-1}. \tag{39}$$

In combination with Eqs. (13) and (15), this yields

$$h \sim q_{\mathrm{i}}^{\frac{1-\alpha}{\psi}} S^{-1}. \tag{40}$$

Inserting the channel slope at the bedrock surface would lead to an unreasonable thickness $h \to \infty$ at locations where $S \to 0$. In turn, using the slope of the ice surface $H + h$ as in original shallow-ice approximation would cost much of the model's simplicity. So we should use a static approximation similar to Eq. (13) where h only depends on q_{i}, but not on S. For a straight profile ($S = \mathrm{const}$), the exponent in Eq. (40) is about 0.23 for $\alpha = 0.3$ and $\psi = 3$. On the other hand, the sliding velocity is constant if the erosion rate is constant along the profile, and then Eqs. (7) and (13) immediately yield $h \sim q_{\mathrm{i}}^{1-\alpha}$. So the exponent is about 0.7 for a uniform erosion rate. A reasonable assumption for the exponent would be somewhere between the two extremes 0.23 and 0.7. However, exponents greater than α imply that glaciers rather thicken than widen downstream (strictly speaking, with increasing ice flux). As this seems to be unrealistic, it makes sense to assume that the exponent is equal to α (here about 0.3), which means that glaciers have a constant thickness-to-width ratio.

https://doi.org/10.5194/esurf-2021-1
Preprint. Discussion started: 22 January 2021

Earth Surface Dynamics Discussions
Open Access
EGU

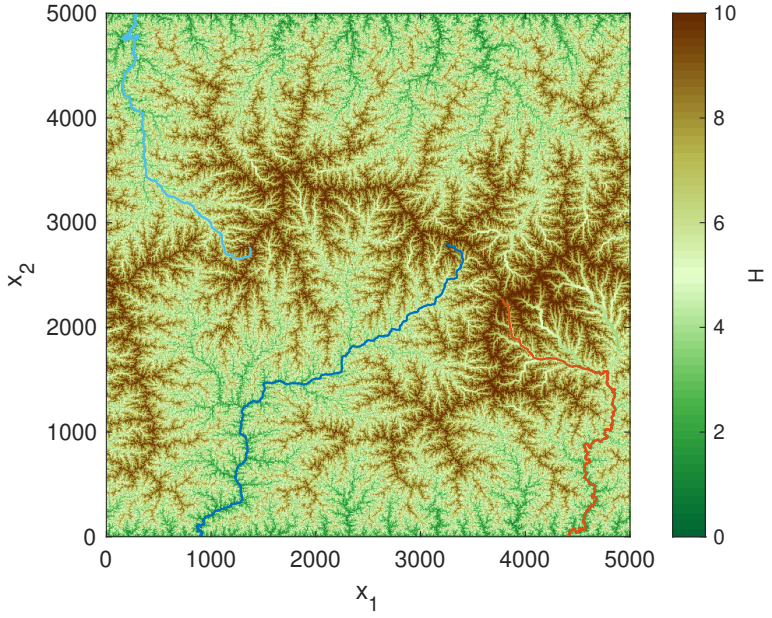

Figure 11. Topography obtained from the shared stream-power model with a thickness-to-width ratio of 0.05 at the time when the ELA reaches $H_e = 8$.

Three effects of the finite thickness can be included in the model. First, the ice surface $H + h$ can be taken into account in the glacial mass balance (Eqs. 21 and 23), as it is usually done in glacial models. Since already H has to be taken at the beginning of the time step in Eq. (23), h is treated the same way without affecting the stability of the scheme strongly.

The most important effect of a finite ice thickness is that the channel slope S should refer to the ice surface $H + h$ instead of the bedrock surface H. Technically, this can be easily implemented by adding h to H before performing the erosion step and subtracting it afterwards. Here the scheme for drawing the swath around the cardinal flow path described in Sect. 3 is particularly useful. It ensures that all points of the swath draining to a given point on the cardinal flow path, except for those located upstream on the cardinal path, have the same prolonged ice flux and thus also the same ice thickness. So the finite ice thickness has only a strong effect within the swath close to the glacier terminus and at confluences where the ice flux changes abruptly. In turn, it sets a higher base level for tributaries at the boundary of the swath, which facilitates the formation of steep walls and hanging valleys. However, local depressions in the ice surface may occur at the boundary of the swath or along the cardinal flow path. These would cause a sediment flux opposite to the direction of the ice flux. In order to avoid this, local depressions in the ice surface should be filled.

Figures 11 and 12 illustrate the effect of these two extensions on the example considered in Sect. 5. All parameters are the same, except that the thickness-to-width ratio is 0.05 in nondimensional coordinates. Using the previously suggested length scales of 50 m horizontally and 250 m vertically, the ratio would be 0.25 in reality.

https://doi.org/10.5194/esurf-2021-1
Preprint. Discussion started: 22 January 2021

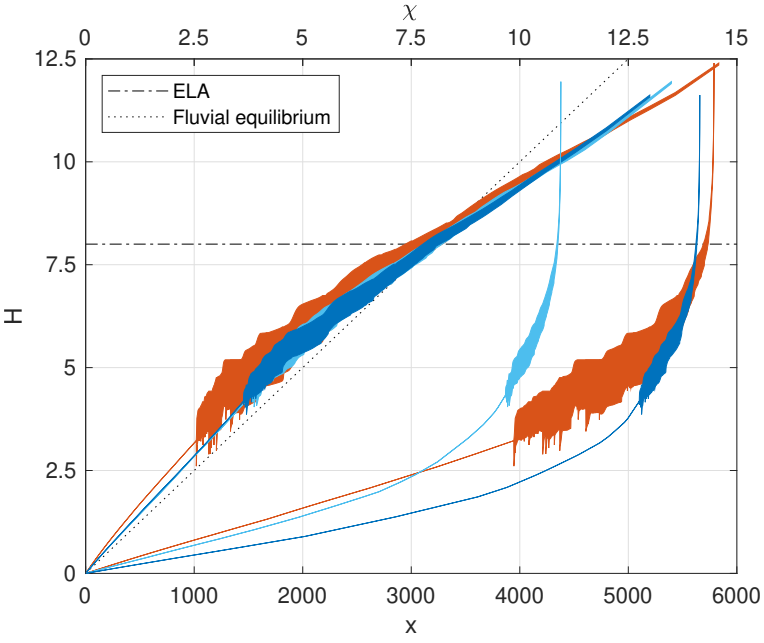

Figure 12. Longitudinal profiles of the largest flow paths in the topography shown in Fig. 11. The filled areas depict the ice layer. The lower set of lines refers to the original longitudinal coordinate x, while the upper set of lines depicts the χ-transformed profiles.

While the slopes along the cardinal flow path are similar to the scenario with zero ice thickness, the glaciers advance further into the valleys here. This difference is related to taking into account the ice surface instead of the bedrock surface in Eq. (23), which defines the part of the precipitation that is converted into ice. This part has increased, which results in a higher ice flux and thus in an advancing of the glaciers.

The upper parts of the glaciated valleys feature smooth segments, which are interrupted by distinct steps. These steps occur at major confluences. Due to the abrupt increase in ice flux at confluences, the ice thickness also increases abruptly. Over long times, however, erosion will smoothen the ice surface, so that the step is transferred from the ice surface to the bedrock topography.

The overdeepening of the valley floor in the lower part of the glacier can be recognized well in the χ-transformed profiles. The longitudinal shape of the bedrock surface looks quite irregular, with several short segments of strong overdeepening. This localized overdeepening occurs if the glacier advances very slowly or the glacier terminus even stays at the same point for some time. The mechanism in the model is the same as for the confluences. Erosion attempts to flatten the steep front, and the gradient of the ice surface is transferred to the bedrock surface. In contrast to the steps at confluences, there is no persistent strong variation in ice flux here. So these local overdeepenings are transient structures which are slowly erased by erosion and filling when the glacier advances further.

The third point where the model could be improved by the finite ice thickness is the separation of the total flow velocity into a deformation velocity v_d and a sliding velocity v_s. While the ice flux (Eq. 7) depends on the sum of both velocities, the erosion

https://doi.org/10.5194/esurf-2021-1
Preprint. Discussion started: 22 January 2021

rate (Eq. 6) depends only on v_s. As discussed in the beginning of Sect. 2, the ratio of the two velocities is proportional to h^2. In the 1-D model of Prasicek et al. (2018), this relation was used for eliminating v_d from the equations. Equation (7) then turns into

$$q_\mathrm{i} = whv_\mathrm{s}\left(1+\beta h^2\right), \tag{41}$$

with a parameter β depending on the rheology of the ice (for details, see Prasicek et al., 2018). The thickness h cannot be eliminated easily then. If we, however, assume that the last term in Eq. (41) is only a small correction, we can insert the estimate of h developed in this section there. Then all subsequent relations remain the same, but where A_i is replaced by

$$\frac{A_\mathrm{i}}{1+\beta h^2} = \frac{A_\mathrm{i}}{1+\xi A_\mathrm{i}^{2\alpha}} \tag{42}$$

with another parameter ξ. So the influence of the ice flux on erosion and sediment transport decreases if deformation becomes relevant. While Eq. (42) could easily be implemented, it introduces an additional parameter and will presumably not yield fundamentally different results. This extension is therefore not considered further in this study.

7 Numerical performance

The concepts developed in the previous sections were implemented in the open-source landform evolution model OpenLEM. A fully implicit scheme for the fluvial shared stream-power model was already available in OpenLEM before (Hergarten, 2020).

The behavior concerning the time increment δt is basically the same as for the fluvial version. Practically, the accuracy is not limited by the accuracy of the implicit scheme itself, but by changes in the flow pattern, which are treated in an explicit way. While the flow directions are the only explicit component in the fluvial version, the glacial mass balance, i.e., the terms H and h in Eq. (23), is also treated in an explicit way in the fluvio-glacial version. This may introduce an additional limitation of the maximum time increment if the climatic conditions change rapidly.

The time-dependent simulations with the declining ELA and the finite ice thickness (Sect. 6) were performed with $\delta t = 10^{-2}$, $\delta t = 10^{-3}$, and $\delta t = 10^{-4}$. On a visual level (Figs. 11 and 12), the results were almost indistinguishable for $\delta t = 10^{-3}$ and $\delta t = 10^{-4}$, while a small difference was observed for $\delta t = 10^{-2}$. However, the difference is rather a small shift on the time axis than a principal difference in the shape of the glaciers and the resulting landforms. So $\delta t = 10^{-3}$ should be a safe choice, while larger values should also be possible if required, e.g., in long-term simulations. If we, e.g., assume a fluvial erodibility of $K = 2.5$ Myr^{-1} (Robl et al., 2017), a unit of nondimensional time corresponds to 400,000 yr. So time increments of some hundred years appear to be safe, while some thousand years will also yield reasonable results.

However, the fluvio-glacial model requires a higher numerical effort per time step than the purely fluvial version. On the 5000×5000 grid, an increase in CPU time by a factor of about 1.7 was found for the fluvio-glacial shared stream-power model compared to the respective fluvial version even if the ice flux is zero everywhere. This factor increases to about 2.7 if the topography is completely glaciated. This factor, however, depends on the width of the glaciers. An increase of the factor of proportionality in Eq. (12) will result in an increasing numerical effort. In principle, the factors may also increase slightly for

https://doi.org/10.5194/esurf-2021-1
Preprint. Discussion started: 22 January 2021

larger grids than the 5000×5000 nodes considered here since the width of the largest glaciers may also increase then. In turn, the implementation in OpenLEM used here is still in a preliminary state and leaves room for further optimization.

So the increase in numerical effort compared to the purely fluvial model is moderate, and simulations even over several million years are possible on standard PCs.

8 Conclusions

This study proposes a stream-power law for glacial erosion, where even the concavity index appears to be the same as for fluvial erosion. This property allows for a seamless combination with fluvial erosion, where erosion by meltwater can also be included conveniently. Sediment transport can also be taken into account with the help of the shared stream-power model recently presented by Hergarten (2020).

Regarding the implementation in a large-scale landform evolution model, the main difference towards fluvial erosion is that glaciers are usually wider than the grid spacing in contrast to rivers. Including the finite width of glaciers is the main challenge in the implementation.

While the first model formulation assumes an infinitely thin ice layer, a finite thickness can also be included, where further approximations are necessary. With this extension, overdeepenings, hanging valleys, and steps at confluences can be simulated in an at least qualitatively reasonable way.

The implementation in the open-source landform evolution model OpenLEM uses the fully implicit scheme for erosion and sediment transport proposed by Hergarten (2020) in the context of fluvial landform evolution. This scheme allows for arbitrary time increments in principle, where changes in the flow pattern practically define an upper limit. The numerical effort is moderately higher than for the purely fluvial version and should be some orders of magnitude lower than for models based on the shallow-ice equations such as ICE-CASCADE and iSOSIA. Simulations even over several million years can be performed on standard PCs.

As a main limitation, the model presented here requires empirical relations for the width and the thickness of glaciers as a function of their ice flux. In contrast, models that implement the shallow-ice approximation directly are able to adjust the geometry of the cross section according to the initial geometry of the valley, its slope, and the parameters of the ice flux. A detailed benchmarking against the iSOSIA model as a reference with regard to the efficiency and to the question how well the stream-power-based model captures glacial erosion will be subject of a subsequent study.

Code and data availability. The open-source landform evolution model OpenLEM including the extensions presented here is freely available at http://hergarten.at/openlem. An additional package that contains all codes and simulated data is available at http://hergarten.at/openlem/esurf-2021-1.zip (preliminary location during the review phase). The author is happy to assist interested readers in reproducing the results and performing subsequent research.

https://doi.org/10.5194/esurf-2021-1
Preprint. Discussion started: 22 January 2021

Earth Surface Dynamics Discussions
Open Access
EGU

425

Competing interests. The author declares that there is no conflict of interest.

https://doi.org/10.5194/esurf-2021-1
Preprint. Discussion started: 22 January 2021

References

Bahr, D. B.: Width and length scaling of glaciers, J. Glaciology, 43, 557–562, https://doi.org/10.3189/S0022143000035164, 1997.

Beaud, F., Flowers, G. E., and Venditti, J. G.: Efficacy of bedrock erosion by subglacial water flow, Earth Surf. Dynam., 4, 125–145, https://doi.org/10.5194/esurf-4-125-2016, 2016.

Braun, J. and Willett, S. D.: A very efficient O(n), implicit and parallel method to solve the stream power equation governing fluvial incision and landscape evolution, Geomorphology, 180–181, 170–179, https://doi.org/10.1016/j.geomorph.2012.10.008, 2013.

Braun, J., Zwartz, D., and Tomkin, J. H.: A new surface-processes model combining glacial and fluvial erosion, Ann. Glaciol., 28, 282–290, https://doi.org/10.3189/172756499781821797, 1999.

Cuffey, K. M. and Paterson, W. S. B.: The Physics of Glaciers, Butterworth-Heinemann, Oxford, 4 edn., 2010.

Davy, P. and Lague, D.: Fluvial erosion/transport equation of landscape evolution models revisited, J. Geophys. Res. Earth Surf., 114, F03 007, https://doi.org/10.1029/2008JF001146, 2009.

Egholm, D. L., Knudsen, M. F., Clark, C. D., , and Lesemann, J. E.: Modeling the flow of glaciers in steep terrains: The integrated second-order shallow ice approximation (iSOSIA), J. Geophys. Res. Earth Surf., 116, F02 012, https://doi.org/10.1029/2010JF001900, 2011.

Egholm, D. L., Pedersen, V. K., Knudsen, M. F., and Larsen, N. K.: Coupling the flow of ice, water, and sediment in a glacial landscape evolution model, Geomorphology, 141–142, 47–66, https://doi.org/10.1016/j.geomorph.2011.12.019, 2012.

Fowler, A. C. and Larson, D. A.: On the flow of polythermal glaciers – I. Model and preliminary analysis, Proc. R. Soc. Lond., 363, 217–242, https://doi.org/10.1098/rspa.1978.0165, 1978.

Guerit, L., Yuan, X. P., Carretier, S., Bonnet, S., Rohais, S., Braun, J., and Rouby, D.: Fluvial landscape evolution controlled by the sediment deposition coefficient: Estimation from experimental and natural landscapes, Geology, 47, 853–856, https://doi.org/10.1130/G46356.1, 2019.

Hack, J. T.: Studies of longitudinal profiles in Virginia and Maryland, no. 294-B in US Geol. Survey Prof. Papers, US Government Printing Office, Washington D.C., https://doi.org/10.3133/pp294B, 1957.

Hallet, B.: A Theoretical Model of Glacial Abrasion, J. Glaciology, 23, 39–50, https://doi.org/10.3189/S0022143000029725, 1979.

Hergarten, S.: Transport-limited fluvial erosion – simple formulation and efficient numerical treatment, Earth Surf. Dynam. Discuss., 2020, 1–16, https://doi.org/10.5194/esurf-2020-39, 2020.

Hergarten, S. and Neugebauer, H. J.: Self-organized critical drainage networks, Phys. Rev. Lett., 86, 2689–2692, https://doi.org/10.1103/PhysRevLett.86.2689, 2001.

Hergarten, S., Robl, J., and Stüwe, K.: Extracting topographic swath profiles across curved geomorphic features, Earth Surf. Dynam., 2, 97–104, https://doi.org/10.5194/esurf-2-97-2014, 2014.

Howard, A. D.: A detachment-limited model for drainage basin evolution, Water Resour. Res., 30, 2261–2285, https://doi.org/10.1029/94WR00757, 1994.

Hutter, K.: Time-dependent surface elevation of an ice slope, J. Glaciology, 25, 247–266, https://doi.org/10.3189/S0022143000010479, 1980.

Lague, D.: The stream power river incision model: evidence, theory and beyond, Earth Surf. Process. Landforms, 39, 38–61, https://doi.org/10.1002/esp.3462, 2014.

Pelletier, J. D.: Minimizing the grid-resolution dependence of flow-routing algorithms for geomorphic applications, Geomorphology, 122, 91–98, https://doi.org/10.1016/j.geomorph.2010.06.001, 2010.

https://doi.org/10.5194/esurf-2021-1
Preprint. Discussion started: 22 January 2021

Perron, J. T. and Royden, L.: An integral approach to bedrock river profile analysis, Earth Surf. Process. Landforms, 38, 570–576, https://doi.org/10.1002/esp.3302, 2013.

Perron, J. T., Dietrich, W. E., and Kirchner, J. W.: Controls on the spacing of first-order valleys, J. Geophys. Res. Earth Surf., 113, F04 016, https://doi.org/10.1029/2007JF000977, 2008.

Prasicek, G., Herman, F., Robl, J., and Braun, J.: Glacial steady state topography controlled by the coupled influence of tectonics and climate, J. Geophys. Res. Earth Surf., 123, 1344–1362, https://doi.org/10.1029/2017JF004559, 2018.

Prasicek, G., Hergarten, S., Deal, E., Herman, F., and Robl, J.: A glacial buzzsaw effect generated by efficient erosion of temperate glaciers in a steady state model, Earth Planet. Sci. Lett., 543, 116 350, https://doi.org/10.1016/j.epsl.2020.116350, 2020.

Rigon, R., Rodriguez-Iturbe, I., Maritan, A., Giacometti, A., Tarboton, D. G., and Rinaldo, A.: On Hack's law, Water Resour. Res., 32, 3367–3374, 1996.

Robl, J., Hergarten, S., and Prasicek, G.: The topographic state of fluvially conditioned mountain ranges, Earth Sci. Rev., 168, 290–317, https://doi.org/10.1016/j.earscirev.2017.03.007, 2017.

Whipple, K. X., DiBiase, R. A., and Crosby, B. T.: Bedrock rivers, in: Fluvial Geomorphology, edited by Shroder, J. and Wohl, E., vol. 9 of *Treatise on Geomorphology*, pp. 550–573, Academic Press, San Diego, CA, https://doi.org/10.1016/B978-0-12-374739-6.00226-8, 2013.

Willgoose, G.: Mathematical modeling of whole landscape evolution, Annu. Rev. Earth Planet. Sci., 33, 443–459, https://doi.org/10.1146/annurev.earth.33.092203.122610, 2005.

Wobus, C., Whipple, K. X., Kirby, E., Snyder, N., Johnson, J., Spyropolou, K., Crosby, B., and Sheehan, D.: Tectonics from topography: Procedures, promise, and pitfalls, in: Tectonics, Climate, and Landscape Evolution, edited by Willett, S. D., Hovius, N., Brandon, M. T., and Fisher, D. M., vol. 398 of *GSA Special Papers*, pp. 55–74, Geological Society of America, Boulder, Washington, D.C., https://doi.org/10.1130/2006.2398(04), 2006.

Yuan, X. P., Braun, J., Guerit, L., Rouby, D., and Cordonnier, G.: A new efficient method to solve the stream power law model taking into account sediment deposition, J. Geophys. Res. Earth Surf., 124, https://doi.org/10.1029/2018JF004867, 2019.